



Wind-induced shear and torsion in low-rise and medium-rise buildings: Provisions of National Building Code of Canada 2015

Journal:	<i>Canadian Journal of Civil Engineering</i>
Manuscript ID	cjce-2017-0107.R1
Manuscript Type:	Article
Date Submitted by the Author:	31-Jul-2017
Complete List of Authors:	Nguyen, Thai Son; Concordia University, Building, Civil and Environmental Engineering Stathopoulos, Ted; Concordia University Tirca, Lucia; Concordia University, Building, Civil and Environmental Engineering
Is the invited manuscript for consideration in a Special Issue? :	N/A
Keyword:	wind loads, code provisions, shear, torsion, low-rise and medium-rise buildings

SCHOLARONE™
Manuscripts

1 **Wind-induced shear and torsion in low-rise and medium-rise buildings:**
2 **Provisions of National Building Code of Canada 2015**

3 Thai Son Nguyen, Ted Stathopoulos, Lucia Tirca

4
5 **T.S. Nguyen.** M.A.Sc. student, Department of Building, Civil, and Environmental Engineering,
6 Concordia University, 1455 De Maisonneuve Blvd. West, Montreal, Quebec, Canada, H3G 1M8.

7 **T. Stathopoulos.** Professor, Department of Building, Civil, and Environmental Engineering, Concordia
8 University, 1455 De Maisonneuve Blvd. West, Montreal, Quebec, Canada, H3G 1M8.

9 **L. Tirca.** ¹Associate Professor, Department of Building, Civil, and Environmental Engineering,
10 Concordia University, 1455 De Maisonneuve Blvd. West, Montreal, Quebec, Canada, H3G 1M8.

11 ¹Corresponding author (e-mail: lucia.tirca@concordia.ca)

12 **Word count: 5982**

13
14
15
16
17
18
19
20
21
22
23
24
25
26
27
28
29
30
31

Draft

32 **Abstract**

33 This paper discusses the shear and torsion induced in low-rise and medium-rise buildings, according to
34 wind load specifications provided in NBCC 2015. Results from experimental studies, carried out in wind
35 tunnels were compared with corresponding NBCC 2015 provisions under different upstream roughness
36 conditions. These comparisons demonstrated notable discrepancies for the case of torsion in low-rise
37 buildings.

38 Further, comparisons between the wind load specifications given in NBCC 2015 and ASCE/SEI 7-10
39 standard were carried out. Following both sets of provisions, wind-induced shear and torsion were
40 computed and compared for five low-rise and medium-rise buildings with the same horizontal dimensions
41 but different heights. Emphasis was directed towards the cases that create maximum shear forces and/or
42 maximum torsions in order to reflect critical design conditions. For low-rise buildings, the ASCE/SEI 7-
43 10 and NBCC 2015 yield similar shear coefficients but quite different torsional coefficients; while for
44 medium-rise buildings, clear agreement was found, for both shear and torsion. The diversity of the results
45 is discussed and some suggestions for improvement of code provisions are made. A definition for
46 medium-rise buildings was provided.

47 **Key words: Wind loads, code provisions, shear, torsion, low-rise and medium-rise buildings**

48 **1. Introduction**

49 Wind loading, especially its torsional effect, plays a critical role on building design. Torsion always
50 occurs even in a perfectly symmetrical building, given that the wind direction toward building wall face is
51 not always perpendicular, and also not distributed uniformly. The equivalent wind force center will not
52 align with the building's center of mass and therefore it will create torsional moments. Moreover, most
53 buildings have inherent eccentricities between the center of mass and that of rigidity. The impacts that
54 wind-induced torsion could cause depend on several conditions, such as: building location, geometry,
55 lateral force-resisting system and its material. Torsion can significantly increase the shear loads applied

56 on the lateral force-resisting system comparing to the conventional loading method, which only considers
57 wind-induced shear. Therefore, the wind torsional effects cannot be neglected and need to be
58 appropriately evaluated by code computations.

59 According to NBCC 2015, low-rise buildings are those with $H \leq 20$ m and $H/D_s < 1$, where H is
60 the building height and D_s is the smaller plan dimension. All buildings with $H > 20$ m and $H/D_s \geq 1$ are
61 classified as high-rise buildings which may be dynamically sensitive or very dynamically sensitive. A
62 building is classified as dynamically sensitive if its lowest natural frequency is less than 1.0 Hz and
63 greater than 0.25 Hz, its height is greater than 60 m, or its height is greater than 4 times its minimum
64 effective width, w . For a rectangular building the minimum effective width is equal to D_s . A building
65 having its lowest natural frequency ≤ 0.25 Hz or its height more than 6 times its minimum effective width
66 is classified as very dynamically sensitive. However, in the current code, there is not a definition for
67 medium-rise buildings. In this study, a medium-rise building is defined as a building with H greater than
68 20 m and less than or equal to 60 m or $1 \leq H/D_s \leq 4$.

69 To investigate the most critical impacts of wind load on medium-rise buildings, along with the
70 conventional full loading case (Case A), three different partial loading cases have been introduced in
71 NBCC 2015 (Cases B, C, D) as shown in Fig. 1. However, several issues have been encountered in the
72 process of determining torsions in load Cases B and D. Firstly, in the torsional load cases, the uniformly
73 distributed wind forces acting on the building are partly reduced (in terms of both magnitude and tributary
74 area) in one or both of the principal directions in order to create the most severe torsional effects on
75 buildings. These effects, along with the effect from the full loading case, are then compared to conclude
76 the most critical scenario in terms of shear and torsional effects. While the subtracted load magnitude is
77 mentioned explicitly in the code, the tributary area remains unclear for load Cases B and D and this
78 creates ambiguities among the NBCC users. Secondly, these load cases do not apply to low-rise
79 buildings, for which the torsional effects are presumably covered by the stipulations of Fig. 2, in which
80 two load Cases, A and B, are specified. However, Stathopoulos et al. (2013) have shown that these
81 provisions may not be adequate for torsion. Although these issues are known for a while, little research

82 has been carried out to address them systematically in order to modify the Canadian wind load
83 specifications accordingly.

84 Other wind codes and standards address torsional loads differently. For instance, the American
85 standard ASCE/SEI 7-10 specifies that, for low-rise buildings, besides applying higher wind loads on
86 wall corners, only 25% of the full design wind pressure is placed on half of the wall face to account for
87 torsional effects. For other buildings, eccentricities and torsion moments are given explicitly by formulas
88 with wind loads applying on full tributary areas for all load cases. In Eurocode (EN 1991-1-4 2005), the
89 torsional effects are taken into account by changing the uniformly distributed wind load in the windward
90 direction represented by rectangular loading to inclined triangular loading while keeping the same load on
91 the leeward wall face. It also regulates that in some cases, wind loads in locations that create beneficial
92 impacts should be completely removed, but this regulation is not very clear for the users. The Australian/
93 New Zealand building code (AS/NZS 1170.2 2011) fully neglects the wind-induced torsion for low-rise
94 and medium-rise buildings whereas for high-rise buildings defined by height > 70.0 m, an eccentricity of
95 20% of the width of windward wall is considered to account for torsion.

96 **2. NBCC 2015 provisions for wind loads on buildings**

97 **2.1 General**

98 The objectives of this study are twofold: i) recommend an approach for determining the appropriate
99 tributary areas needed to generate the maximum torsion effects in Case B and Case D recommended in
100 NBCC 2015 for high-rise buildings and applied herein also for medium-rise buildings and ii) examine the
101 adequacy of wind loads (base shear and torsion) determined by the NBCC 2015 through comparisons
102 with results from previous studies and ASCE/SEI 7-10 standard provisions.

103 The full wind external pressure in NBCC 2015 is given by:

$$p = I_w q C_e C_t C_g C_p \quad (1)$$

104 where I_w is the importance factor for wind load; q is the reference velocity pressure; C_e , C_t and C_g are the
105 exposure, topographic, and gust effect factor; and C_p is the external pressure coefficient. After the wind

106 pressures are acquired they are multiplied by the corresponding projected/ tributary area to attain the
 107 external wind forces acting on the building wall faces. The wind loads are computed for each floor before
 108 being summed up to obtain the base shear. The process is carried out for two orthogonal directions.
 109 Torsion moments are formed by the unbalance of wind pressures on building wall faces, as specified in
 110 the partial loading cases.

111 For buildings higher than 60 m or the height to minimum effective width ratios > 4.0 or with
 112 lowest natural frequency lower than 1.0, the dynamic procedure should be applied. The same provisions
 113 to static procedure, including the partial loading cases, shall be followed, except that the exposure factor,
 114 C_e and the gust factor, C_g are evaluated differently (NBCC 2015). The lowest natural frequency of the
 115 building is recommended to be computed by the following equation:

$$f_n = \frac{1}{2\pi} \sqrt{\frac{\sum_{i=1}^N F_i \frac{x_i}{x_N}}{x_N \sum_{i=1}^N M_i \left(\frac{x_i}{x_N}\right)^2}} \quad (2)$$

116 where N is the number of stories; F_i, M_i are the lateral load and floor mass at level i^{th} ; x_i and x_N are the
 117 horizontal deflections of floor at level i and N , respectively.

118 In some cases, partial loadings can cause severe effects. As already mentioned for high-rise/
 119 medium-rise buildings, four load cases are presented in NBCC 2015 (A, B, C and D). While Cases A and
 120 C focus on the effect of shear force, Cases B and D emphasize the torsional impact on structures. The
 121 conventional loading method is followed by the Case A when 100% of wind forces are loaded separately
 122 in each principal axis. Clearly, this case is found to produce the maximum base shear. The wind loads
 123 with the same magnitude are applied on parts of the wall faces to create additional torsions in load Case
 124 B. The tributary area of the wind pressure acting on a given story wall face is given as a product of the
 125 height of the story under consideration and the horizontal distribution length of the wind load. However,
 126 the latter is not provided explicitly by NBCC 2015, which may lead practitioners to different tributary
 127 areas, and therefore, different wind forces, and potential false assessments of the torsional effects of wind
 128 loads on buildings. Thus, this issue requires clarification. Wind blowing diagonally to the walls can be

129 illustrated equivalently by simultaneous reduced forces. For instance, 75% of full load are applied
130 simultaneously on both wall faces to create Case C. In Case D, 50% of those in Case C are partly
131 subtracted from wall faces. Similar to Case B, the wind projected area in Case D is just mentioned as
132 “reduced from part of projected area”. The term “part” needs to be clarified as it raises questions among
133 the code users.

134 Two load cases are mentioned in NBCC 2015 for low-rise buildings, namely load Case A and
135 Case B, which simulate wind loads applying perpendicular and parallel to the ridge of a building,
136 respectively. As specified in Case B, when acting parallel to the building’s ridge, wind forces also create
137 impacts to both sides of the buildings. Also, the wind pressures are different on opposite sides of the
138 building roof. However, the current study only considers buildings with flat roofs. Therefore, these effects
139 can be neglected because the across-wind forces on opposite wall faces eliminate each other. As a result,
140 the two load cases merge into a single case. The wind pressures are defined as shown in Eq. (1).
141 However, for low-rise buildings, instead of determining the external pressure coefficient, C_p , and gust
142 effect factor, C_g separately as in the case of medium-rise buildings, the external peak composite pressure-
143 gust coefficients, $C_p C_g$ are obtained based on the positions of wind loads applied on the wall faces. The
144 other parameters (I_w , q , C_e) are computed in the same way as for high-rise/ medium-rise buildings.

145 **2.2 Torsional load case for medium-rise buildings**

146 In medium-rise buildings, torsional effects are computed by considering the two partial loading cases:
147 Case B and Case D. The tributary area of wind load that could produce the maximum torsions are
148 recommended by using a mathematical method. The method of determining maximum torsion in Case D
149 is illustrated in Fig. 3. The same approach can be adopted to determine the maximum torsion in load Case
150 B, as it is a simplified case of Case D.

151 As previously mentioned, the tributary area of the uniformly distributed wind force acting on a
152 given story is given as: $A = l \times h$, where h is the height of the story under consideration, and l is the
153 horizontal distribution length of the wind load. According to NBCC 2015, the horizontal distribution

154 length (mentioned as a , b , c and d in Fig. 3) are unknown. These values need to be determined so that the
 155 corresponding wind forces applied simultaneously in both wall faces of the building create a maximum
 156 moment M , which is the summation of the moments induced by wind forces in each direction:

$$M = M_x + M_y \quad (3)$$

157 Herein, M is maximum when M_x and M_y reach their highest values. The moment due to wind load along
 158 the N-S direction is given by:

$$M_x = p_2 b h e_2 - p_1 a h e_1 \quad (4)$$

159 where p_1 and p_2 are uniform wind forces acting on the wall faces in the N-S direction; e_1 and e_2 are the
 160 eccentricities of p_1 and p_2 , respectively; and a and b are the horizontal distribution length of p_1 and p_2 ,
 161 respectively.

162 The eccentricities e_1 and e_2 are: $e_1 = L/2 - a/2$, $e_2 = L/2 - b/2$, where $a = L - b$. By
 163 substituting these parameters in Eq. (4), it results:

$$\begin{aligned} M_x &= p_2 b h \left(\frac{L}{2} - \frac{b}{2} \right) - p_1 a h \left(\frac{L}{2} - \frac{a}{2} \right) = p_2 b h \frac{L}{2} - p_2 h \frac{b^2}{2} - p_1 a h \frac{L}{2} + p_1 h \frac{a^2}{2} \\ &= p_2 b h \frac{L}{2} - p_2 h \frac{b^2}{2} - p_1 (L - b) h \frac{L}{2} + p_1 h \frac{(L - b)^2}{2} \\ &= p_2 b h \frac{L}{2} - p_2 h \frac{b^2}{2} - p_1 h \frac{L^2}{2} + p_1 b h \frac{L}{2} + p_1 h \frac{b^2 + L^2 - 2Lb}{2} \\ &= p_1 h \frac{b^2}{2} - p_2 h \frac{b^2}{2} + p_2 b h \frac{L}{2} - p_1 b h \frac{L}{2} \\ &= \left(\frac{p_1}{2} - \frac{p_2}{2} \right) b^2 h + \left(\frac{p_2 L}{2} - \frac{p_1 L}{2} \right) b h \end{aligned} \quad (5)$$

164 As can be seen, M_x is a quadratic function of variable b . This function reaches its maximum value when
 165 its differentiation with respect to b is equal to zero, i.e.:

$$\begin{aligned} M'_x &= (p_1 - p_2) b h + 0.5(p_2 - p_1) L h = 0 \\ \Leftrightarrow b &= \frac{L}{2} \end{aligned} \quad (6)$$

166 Therefore, the maximum torsion due to wind along the N-S direction occurs at $b = a = L/2$. Similarly,
167 M_y is maximum when $c = d = B/2$.

168 Applying the same procedure, the torsions in Case B are maximum when pressures are applied on
169 half of the wall faces. The maximum torsion effect is chosen by comparing the results of Case B and Case
170 D. The most critical shear effect comes from the maximum value of Case A and Case C.

171 2.3 Torsional load case for low-rise buildings

172 In terms of low-rise buildings, only two Cases, namely A and B, are present in NBCC 2015, when torsion
173 is caused by a higher concentration of wind loads in each wall face corner. As opposed to partial loading
174 cases for medium-rise buildings, the tributary areas of wind forces are stated explicitly for low-rise
175 buildings as exhibited in Fig. 4. Torsion moment for these cases is computed by the following formula:

$$M = (p_1 + p_4)e_1(L - y)h - (p_{1E} + p_{4E})e_{1E}yh \quad (7)$$

176 Herein, y is the width of the end-zone computed as the greater of 6 m and $2z$, where z is the lesser of 10%
177 of the least horizontal dimension or 40% of height, H , but not less than 4% of the least horizontal
178 dimension or 1.0 m.

179 3. Comparisons between NBCC 2015 and experimental results from previous studies

180 3.1 Selection of experimental studies from the literature

181 The first comparisons are made between the wind loads computed by NBCC 2015 and those from wind
182 tunnel tests collected from four previous studies regarding both low-rise and medium-rise buildings under
183 different exposures. The four previous studies chosen are: Isyumov and Case (2000), Keast et al. (2012),
184 Tamura et al. (2003), and Stathopoulos et al. (2013). The configurations of buildings tested in these
185 studies are shown in Table 1, where they are also grouped into low-rise and medium-rise categories.
186 Some assumptions have been made due to the lack of information that is essential for the application of
187 the NBCC 2015 provisions. For instance, the studied buildings are steel structures and the lateral force-
188 resisting systems consist of limited ductility concentrically braced frames. The two largest shear in the

189 two principal wall face directions along with the maximum torsion are selected in each building
 190 considering all load cases, for both low-rise and medium-rise buildings in open and urban-terrain areas.
 191 Four partial loading cases are considered for medium-rise buildings. For the torsional load Cases B and
 192 D, the tributary area has been determined as recommended previously in Eq. (6). For low-rise buildings,
 193 shear and torsion are attained following Cases A and B as prescribed in Fig. 4. Based on building
 194 properties (geometry, dimensions, and natural frequency), some are computed by the static procedure,
 195 while others follow the dynamic procedure. Detailed information about computational procedure for all
 196 buildings is provided in Table 2. It is noted that w parameter provided in Table 2 is the minimum effective
 197 width. For the current study, the ETABS software (CSI 2016) was used to compute the building's natural
 198 frequency.

199 3.2 Shear and torsional coefficients

200 In order to compare results between studies with different building locations and exposure terrains,
 201 maximum base shear forces and torsions are normalized to obtain the shear and torsional coefficients,
 202 defined as follows:

$$C_V = \frac{V}{q_H B L} \quad (8)$$

$$C_T = \frac{T}{q_H B^2 L} \quad (9)$$

$$q_H = q C_e \quad (10)$$

203 where C_V and C_T are shear and torsional coefficients; V and T are the base shear and torsion; B and L are
 204 the shorter and longer horizontal dimensions of the building; q_H is the mean dynamic wind pressure at
 205 roof height H ; q is the reference velocity pressure based on the mean hourly wind speed; and C_e is the
 206 exposure factor.

207 Due to the diversity of coefficient definitions among the past studies, all coefficients given have
208 all been transformed to be consistent with those of the current study. The transformation equations used
209 for each study are provided in Table 3.

210 3.3 Results and Discussions

211 In this section, the comparisons between the shear and torsional coefficients resulted from wind tunnel
212 tests and the corresponding code results are depicted in graphs where the vertical axis shows shear or
213 torsional coefficients from wind tunnel tests, while those from NBCC 2015 are placed on the horizontal
214 axis. Each pair of results (experimental and code results) is represented by a point. The closer the point is
215 to the balance line (form an angle of 45^0 with the axes), the better is the agreement between code
216 provisions and experimental results.

217 Figure 5 compares the torsional coefficients in two separate categories namely low-rise and
218 medium-rise buildings. Clearly, the NBCC 2015 greatly underestimates torsional effects on low-rise
219 buildings through all cases. Thus, all points shown in the graph for low-rise buildings are at noticeable
220 distances to the balance line (experimental results are 6 to 10 times higher than those from NBCC 2015).
221 Moreover, the underestimation in torsional effects of NBCC 2015 for low-rise buildings can be witnessed
222 through the case of the two buildings of Stathopoulos et al. (2013). These two buildings are 20.0 m high
223 (low-rise building) and 30.0 m high (medium-rise building) and have the same horizontal dimensions and
224 exposure conditions. According to the Canadian code computations, the torsional coefficient increases ten
225 times from 0.024 (20.0 m – low-rise building) to 0.26 (30.0 m - medium-rise building). The values from
226 the wind tunnel tests are 0.15 and 0.27, correspondingly, making a smaller jump of about 1.8 times. For
227 medium-rise buildings, all studies give similar results with the computations from NBCC 2015, except for
228 the case of the building of Tamura et al. (2003) in urban-terrain area where the results are overestimated.
229 Furthermore, the NBCC 2015 have resulted slightly higher torsional coefficient values.

230 In conclusion, torsional effects on low-rise buildings are not assessed properly by NBCC 2015.
231 Conversely, good assessments have been shown in medium-rise buildings with the application of partial

232 loading. Therefore, it was decided to test the effectiveness of the medium-rise building methodology for
233 low-rise buildings although, according to NBCC 2015, partial loading cases are not required for them.
234 Cases B and D are applied to all the low-rise buildings of the previous studies to obtain the maximum
235 torsions. The torsional coefficients resulted from this process are exhibited in Fig. 6. The abbreviation
236 “PL” in the figure implies the results from the partial loading Cases B and D. Much better results are
237 shown clearly as the torsional coefficients of the code are much closer to those provided by the
238 experimental studies. Discrepancies decrease to only within 1.5 times. Evidently, if partial loading cases
239 are applied as for the case of medium-rise buildings, the torsional effects on low-rise buildings can be
240 estimated more appropriately, although somewhat underestimated.

241 Figure 7 presents the comparisons between shear coefficients obtained from NBCC 2015 and
242 wind tunnel tests. The shear coefficients are computed in two principal wind directions: N-S and W-E. In
243 general, good similarities between the code computations and the test results are present. For low-rise
244 buildings, four out of six shear coefficients computed from NBCC 2015 are nearly equal to the
245 experimental coefficients. However, an underestimating trend is demonstrated. Additionally, shear
246 coefficients adequacy decrease in the N-S direction (the longer wall face). For medium-rise buildings,
247 there is an excellent agreement in seven out of eight cases. The best agreement is found in the results of
248 Stathopoulos et al. (2013) for both terrains (only roughly 1% difference). The largest difference found
249 was approximately 16%, in the case of the 60.0 m high building in the study of Keast et al. (2012), which
250 is also the highest building among all studies.

251 In brief, with the exception of the underestimated torsional effects for low-rise buildings, the
252 NBCC 2015 seem to evaluate the impact of wind loads on low-rise (shear effects) and medium-rise
253 buildings adequately. Potential remedies can be taken in the case of torsional effects on low-rise buildings
254 by applying the partial loading cases, similar to the case of medium-rise buildings.

255 **3.4 Discussion on the discrepancies between results from NBCC 2015 and wind tunnel tests**

256 The underestimation in torsions for low-rise buildings is due to the fact that the code does not take partial
 257 loading into account. As can be seen in Fig. 2, the higher wind pressures (the factor that produces the
 258 torsional effects) are only placed in a small area $y \times h$ in the building's corners, where y is the maximum
 259 of 6 m or $2z$. This value, in most cases, is not comparable to half of the wall dimension perpendicular to
 260 wind directions, which is shown in Eq. (6) to produce the maximum torsion. This inappropriate pressure
 261 distribution also results in small shear coefficients, as illustrated in Fig. 7.

262 Discrepancies between shear and torsional coefficients in medium-rise buildings provided by
 263 NBCC 2015, as shown in Figs. 5, 6 and 7, may be attributed to the lowest natural frequency of the
 264 building, f_n . As shown in Table 1, the dynamic procedure was applied for all medium-rise buildings.
 265 Wind loads determined by dynamic procedure are controlled by the building natural frequency, which
 266 may be not similar between buildings in the current study and the previous studies due to the differences
 267 in building materials and lateral force-resisting systems. The assumptions made in the current study may
 268 result in different building material, lateral force-resisting system, and damping ratios to the past studies.
 269 As a result, dissimilar natural frequencies between buildings occur and directly affect the values of the
 270 size reduction factor s , and gust energy ratio at the natural frequency of the structure F , and consequently
 271 the gust factor C_g as shown below:

$$C_g = 1 + g_p \sqrt{\frac{K}{C_{eH}} \left(B + \frac{sF}{\beta} \right)} \quad (11)$$

$$s = \frac{\pi}{3} \left[\frac{1}{1 + \frac{8f_n H}{3V_H}} \right] \left[\frac{1}{1 + \frac{10f_n W}{V_H}} \right] \quad (12)$$

$$F = \frac{(1220f_n/V_H)^2}{[1 + (1220f_n/V_H)^2]^{4/3}} \quad (13)$$

272 Herein, g_p is the peak factor, K is a factor related to the surface roughness coefficient of the terrain, C_{eH} is
 273 the exposure factor evaluated at the top of the building, B is the background turbulence factor, β is the
 274 critical damping ratio in the along-wind direction, f_n is the fundamental frequency, H is the height of the

275 building, V_H is the mean wind speed at the top of the structure, and w is the effective width of windward
 276 face of the building.

277 Computations with steel and concrete structures with different types of lateral force-resisting
 278 system were carried out to examine the differences between their wind-induced shears and torsions. The
 279 30.0 m height building of Stathopoulos et al. (2013) is taken as an example. As mentioned previously, the
 280 building in this current study is a steel structure with limited ductility concentrically braced frames as
 281 lateral force-resisting systems. Two other cases were considered for the comparison purposes, as the
 282 buildings were assumed to be moment resisting frame concrete structure and concrete building without a
 283 lateral force-resisting system. These buildings were designed for gravity and seismic loads, as well as, a
 284 structural analysis software was used to determine the fundamental frequencies of these buildings.

285 The three buildings have different damping ratio values, ranging from 2% to 5%, and natural
 286 frequencies ranging from 0.5 Hz to 1.0 Hz. Although they produce different gust factors C_g , similar
 287 torsional coefficients were found for the steel braced-frame building, the concrete building with moment
 288 resisting frame and the concrete building without lateral force-resisting system (0.37, 0.369, and 0.35,
 289 respectively). In addition, the corresponding shear coefficients computed in both directions were almost
 290 identical. Clearly, although building material and lateral force-resisting system directly affect the wind-
 291 induced shear and torsion of a building, the differences that they create are not significant.

292 4. Comparisons between ASCE/SEI 7-10 and experimental results from previous studies

293 This section presents similar comparisons with those illustrated previously in Figs. 5 and 7. The same
 294 buildings were considered using the ASCE/SEI 7-10 standard. Two different procedures, namely
 295 Directional and Envelope, are available in ASCE/SEI 7-10 to determine the wind loads. The Directional
 296 procedure can be applied to buildings of all heights, while the Envelope procedure is specified only for
 297 low-rise buildings. The wind pressure, following the Directional and Envelope procedures, are as follows:

$$p = qGC_p - q_i(GC_{pi}) \text{ (Directional)} \quad (14)$$

$$p = q_h[(GC_{pf}) - (GC_{pi})] \text{ (Envelope)} \quad (15)$$

298 where q is the velocity pressure evaluated at height z above the ground for windward walls and at height h
299 for leeward walls, q_h and q_i are the velocity pressure evaluated at mean roof height h , G is the gust factor,
300 C_p is the external pressure coefficient, (GC_{pi}) is the peak internal pressure coefficient, and (GC_{pf}) is the
301 peak external pressure coefficient. Because it is assumed in the current paper that all buildings under
302 consideration are enclosed, the internal pressure effects have been neglected, since they cancel each other
303 on opposite walls.

304 The ASCE/SEI 7-10 specifies four partial loading cases for the Directional procedure, and four
305 cases for the Envelope procedure (including two torsional load cases), as shown in Figs. 8 and 9,
306 respectively. Clearly, Cases 1 and 3 of the Directional Procedure are similar to NBCC 2015, but a
307 difference can easily be witnessed in the torsional load cases (Cases 2 and 4). In these cases, the same
308 approach as Cases B and D (see Fig. 9) is used, except that a torsion M_T is defined explicitly and the wind
309 pressure is distributed uniformly over the full tributary area of the building wall face. In terms of low-rise
310 buildings, two additional torsional load cases are added to the Envelope procedure besides two
311 conventional load cases as similar to NBCC 2015. In these additional cases, only 25% of the full wind
312 pressures are applied to half of the building wall, while the rest remain unchanged as the conventional
313 case, which in turn creates a greater amount of torsion comparing to the Canadian provisions.

314 For low-rise buildings, maximum base shears and torsions are obtained by considering both
315 Directional and Envelope procedures. While the maximum base shears are determined by Case 1 of the
316 Directional procedure, the torsional effect is found to be maximum in Case B (torsion) of the Envelope
317 procedure. For medium-rise buildings, only the Directional procedure is carried out, where Case 1 creates
318 the maximum shear forces. At the same time, the most severe torsional case is determined by either Case
319 2 or Case 4. After the maximum base shears and torsions have been obtained for all buildings, shear and
320 torsional coefficients are computed following Eqs. (8) and (9).

321 All the ASCE/SEI 7-10 values are multiplied by 1.53^2 due to the difference between the 3-second
322 and 1-hour wind speed used in NBCC 2015 and ASCE 7-10, respectively. Particularly, the wind speed in
323 NBCC 2015, measured over a period of 1 hour, is 1.53 times smaller than that of the ASCE/SEI 7-10,
324 which is calculated over a period of 3 seconds (Durst 1960).

325 Figure 10 shows similar torsional coefficient values computed from experimental tests reported in
326 past studies and those computed according to ASCE/SEI 7-10 provisions. For low-rise buildings, the
327 American standard has generated almost the same results as the experimental values on three out of four
328 studies. The study of Tamura et al. (2003) in urban terrain is the only one that gives a notable
329 discrepancy.

330 Better agreements have been illustrated in the results for medium-rise buildings. The highest
331 difference is from the study of Stathopoulos et al. (2013), where an experimental coefficient is found
332 equal to 75% of that from the American provision. Other findings are very similar: experimental results
333 are roughly 95% of code computations.

334 Figure 11 compares shear coefficients for low-rise and medium-rise buildings obtained using the
335 ASCE/SEI 7-10 provisions and the respective wind tunnel results. Generally, the discrepancies induced in
336 low-rise buildings are slightly higher than those in medium-rise buildings. All points shown in the graph
337 of medium-rise buildings almost overlap with the 45° line. Stathopoulos et al. (2013) have again given
338 identical values to those provided by the American standard. This resemblance tendency has been
339 previously identified in the case of NBCC 2015 and plotted in Fig. 7. In terms of low-rise buildings,
340 overestimated results were found in the comparisons with Tamura et al. (2003) building in open terrain.
341 This is possible due to the differences in the definition of open terrain used in both cases.

342 Overall, the ASCE/SEI 7-10 provisions have given analogous shear results comparing to the wind
343 tunnel results.

344 5. Shear and torsion coefficients in NBCC 2015 and ASCE/SEI 7-10 provisions

345 In this section, the NBCC 2015 and ASCE/SEI 7-10 wind provisions are applied to five buildings, with
346 the same horizontal dimensions but different heights ranging from 14.8 m (low-rise building) to 43.6 m
347 (medium-rise building). The building heights ascend in a step of 7.2 m. The typical plan and elevation
348 views of the five buildings are presented in Fig. 12, where B and L are the shorter and longer horizontal
349 dimensions. Based on these buildings' configurations and natural frequencies, the wind static procedure is
350 applied for low-rise buildings and the dynamic procedure is applied for medium-rise buildings (see Table
351 2). All partial loading cases are carried out to seek the highest wind-induced shears and torsions provided
352 by both codes. The results are shown in Fig. 13.

353 According to NBCC 2015 provisions, the static procedure is applied for the low-rise building
354 (14.8 m), while the medium-rise buildings are computed with the dynamic procedure. Similar to the
355 previous sections, Cases B and D are carried out with the wind tributary area determined following Eq.
356 (6). Very small torsional coefficient is produced from the low-rise building. Thus, the torsional coefficient
357 rises immensely when building class changes from low-rise to medium-rise building (14.8 m to 22.0 m)
358 and can be witnessed easily from the sudden change in the C_T line's alignment in Fig. 13. Moreover, this
359 jump seems to be noticeably high comparing to the average of 1.3 resulted for the same height steps
360 which are: 22.0 m to 29.2 m, 29.2 m to 36.4 m and 36.4 m to 43.6 m. In terms of shear coefficients, the
361 differences are apparently less remarkable. In the N-S direction, the difference between the low-rise and
362 medium-rise buildings is just slightly greater than that between two medium-rise buildings with
363 consecutive heights and decreases largely when it comes to the W-E direction.

364 Through the good agreement with experimental values (Fig. 10), the ASCE/SEI 7-10 wind
365 provisions are believed to have successfully predicted the wind effects and can be considered a good
366 reference to evaluate the adequacy of other codes. Therefore, the coefficients found in NBCC 2015 are
367 compared with the values provided by the ASCE/SEI 7-10 provisions on the same set of buildings.
368 Significant discrepancies are found regarding torsional coefficients, especially in the case of low-rise
369 buildings. Firstly, the torsional coefficient provided in NBCC 2015 for low-rise buildings is much smaller
370 than that of ASCE/SEI 7-10, implying a serious underestimation of NBCC 2015 in evaluating the wind-

371 induced torsional effects on low-rise buildings. Secondly, for medium-rise buildings, NBCC 2015 has
372 provided torsional coefficients roughly 1.5 times higher than those of ASCE/SEI 7-10. Additionally, this
373 trend increases with the building height and is greater than the 6% difference shown in Figs. 5 and 10
374 where the same computations were made for smaller buildings. Indeed, the longer horizontal dimension
375 of the buildings in this section (150.5 m) is more than double the maximum dimension from the previous
376 comparisons (61.0 m). Therefore, it can be concluded that the recommended tributary area is conservative
377 for determining the torsional effects of large and high buildings.

378 Conversely, in terms of shear coefficients, Fig.13 shows that both codes have given similar results
379 regardless of building height. Thus, although the discrepancies fluctuate with the ascending building
380 heights, the two codes only give differences within 10%. Excluding the results of low-rise buildings, all
381 shear coefficients resulted from the NBCC 2015 are higher than those from the ASCE/SEI 7-10. It is also
382 noticeable that the gap between the shear coefficients computed for the low-rise building (14.8 m height)
383 and those for the 22.0 m high building (medium-rise) is significantly higher comparing to the difference
384 between the other medium-rise buildings. For example, the shear coefficients of the 14.8 m high building
385 in both orthogonal directions are on average about 50% of those of the 22.0 m high building. The average
386 between the other medium-rise buildings is almost 80%. However, this difference does not imply any
387 underestimation in shear computations in low-rise buildings as similar trend between code provisions and
388 wind tunnel test results has been found in previous sections.

389 **6. Recommendations**

390 Some recommendations are made here to improve the adequacy of the NBCC 2015 provisions in terms of
391 torsional effects.

392 For low-rise buildings, according to Fig. 6, the application of wind partial loading cases into low-
393 rise buildings has significantly improved the torsion assessments of NBCC 2015, although some
394 discrepancies still occur. However, by adding two torsional load cases and distributing the wind pressure
395 on building faces differently from NBCC 2015, the American standard provisions have yielded closer

396 coefficients to results from wind tunnel tests (Figs. 10 and 11). Therefore, it is recommended that the
397 torsion methodology provided by ASCE/SEI 7-10 for low-rise buildings to be applied to the NBCC 2015.

398 For medium-rise buildings, by applying the wind pressure on half of the wall area (Eq. 6), Case B and
399 Case D have resulted in adequate torsions (Fig. 5). However, when the building horizontal dimensions
400 and height increase, this method can provide conservative results with an increasing trend, as can be seen
401 in Fig. 13. Meanwhile, the ASCE/SEI 7-10 standard can provide more appropriate results regardless of
402 building configurations, as is indicated through the comparisons with experimental coefficients in Fig. 10.
403 Consequently, the adequacy of torsional results in medium-rise buildings can be improved in the NBCC
404 2015 provisions by explicitly defining an additional moment and eccentricity in each torsional loading
405 case as in the ASCE/SEI 7-10.

406 7. Summary and Conclusion

407 Results from previous wind tunnel tests have shown that the NBCC 2015 provides adequate assessment
408 of wind effects on low-rise and medium-rise buildings with the only exception of torsional effects on low-
409 rise buildings, which are underestimated significantly. Load cases B and D, available for medium-rise
410 buildings, have been applied, and yielded improved results, although still low compared to the
411 experimental results.

412 Through the comparisons with ASCE/SEI 7-10, good agreement in shear computations has been
413 found between the two sets of provisions. For medium-rise buildings, if the wind loads are placed on half
414 of the building wall in Case B and Case D, appropriate results can be obtained from the NBCC 2015
415 although conservative torsions may arise when the building horizontal dimensions and height raise. The
416 comparisons also show that the torsional effects evaluated by NBCC 2015 for low-rise buildings are
417 seriously underestimated.

418 In conclusion, it is suggested that the ASCE/SEI 7-10 torsion methodology to be applied in future
419 editions of NBCC for both low-rise and medium-rise buildings in order to attain appropriate torsional
420 evaluations.

421 **Acknowledgments**

422 The authors would like to acknowledge the financial support of the Québec Fonds pour la Recherche sur
423 la Nature et les Technologies (FQRNT) for the Centre d'Études Interuniversitaires des Structures sous
424 Charges Extrêmes (CEISCE).

425

426

427 **References**

428 ASCE/SEI 7-10. 2010. Minimum design loads for buildings and other structures. Structural Engineering
429 Institute of ASCE, Reston, VA.

430 AS-NZS 1170-2. 2011. Structural design actions – Part 2: Wind actions (By Authority of New Zealand
431 Structure Verification Method B1/VM1).

432 Computer and Structure, Inc., USA. 2016. CSI Analysis Reference Manual for ETABS.

433 Durst, C.S. 1960. Wind speeds over short periods of time. Meteor. Mag. 89, 181-187.

434 EN 1991-1-1. 2005. Eurocode 1: Actions on structures – Part 1-4: General actions – Wind actions.

435 Isyumov, N. and Case, P.C. 2000. Wind-induced torsional loads and responses of buildings, Proceedings
436 of Structures Congress, Philadelphia, Pennsylvania, USA, Sponsored by ASCE/SEI, May 8-10.

437 Keast, D.C., Barbagallo, A., Wood, G.S. 2012. Correlation of wind load combinations including torsion
438 on medium-rise buildings. Wind and Structures, An International Journal, 15(5), 423-439.

439 National Research Council of Canada. 2015. *National Building Code of Canada - Part 4*.
440 Ottawa, On.

441 Stathopoulos, T., Elsharawy, M., Galal, K. 2013. Wind load combinations including torsion for
442 rectangular medium-rise buildings. Int. J. of high-rise buildings. Sept. 2013, Vol. 2, no. 3, 245-255.

443 Tamura, Y., Kikuchi, H., Hibi, K. 2003. Quasi-static wind load combinations for low- and middle-rise
444 buildings. Journal of Wind Engineering and Industrial Aerodynamics, 91, 1613-1625.

445

446

447

448

449

450

451

452 **List of figure captions**

453 **Fig. 1:** Load cases for medium-rise buildings after NBCC 2015.

454 **Fig. 2:** Load cases for low-rise buildings after NBCC 2015.

455 **Fig. 3:** Load Case D for medium-rise buildings analyzed in x and y directions.

456 **Fig. 4:** Load cases for low-rise flat roof buildings according to NBCC 2015 provisions.

457 **Fig. 5:** Comparison of torsional coefficients for low-rise and medium-rise buildings in NBCC 2015 with
458 experimental results from previous studies.

459 **Fig. 6:** Comparison of torsional coefficients for low-rise in NBCC 2015 (following partial loading cases,
460 PL) with experimental results from previous studies.

461 **Fig. 7:** Comparison of shear coefficients for low-rise and medium-rise buildings in NBCC 2015 with
462 experimental results from previous studies.

463 **Fig. 8:** Partial loading case for the Directional procedure after ASCE/SEI 7-10.

464 **Fig. 9:** Partial loading cases for the Envelope procedure after ASCE/SEI 7-10.

465 **Fig. 10:** Comparison of torsional coefficients for low-rise and medium-rise buildings in ASCE/SEI 7-10
466 with experimental results from previous studies.

467 **Fig. 11:** Comparison of shear coefficients for low-rise and medium-rise buildings in ASCE/SEI 7-10 with
468 experimental results from previous studies.

469 **Fig. 12:** Common plan and elevation views of the buildings in the current study.

470 **Fig. 13:** Shear and torsional coefficients according to NBCC 2015 and ASCE/SEI 7-10.

471

472

473

474 **List of table caption**

475 **Table 1:** Building dimensions and exposure condition.

476 **Table 2:** Computation procedure for the buildings in the previous and current studies according
477 to NBCC.

478 **Table 3:** Original and transformed definition of shear and torsional coefficients in previous
479 studies.

Draft

Tables

Table 1: Building dimensions and exposure conditions.

Study name		Isyumov and Case (2000)	Tamura et al. (2003)	Keast et al. (2012)	Stathopoulos et al. (2013)
Type of building exposure in experiments		Urban	Urban/Open	Open	Open
Low-rise buildings	B (m)	9.75	30		39
	L (m)	29.26	42.5		61
	H (m)	4.88	12.5		20
Medium-rise buildings	B (m)				39
	L (m)				61
	H (m)				30
	B (m)		25	20	39
	L (m)		50	40	61
	H (m)		50	60	40

Table 2: Computation procedure for the buildings in the previous and current studies according to NBCC.

Study	f_n	H/w	H (m)	Procedure
Computation procedure for the buildings in the previous studies according to NBCC				
Isyumov and Case (2000)	4.10	0.50	4.88	Static
Tamura et al. (2003)	1.60	0.42	12.5	Static
	0.40	2.00	50	Dynamic
Keast et al. (2012)	0.33	3.00	60	Dynamic
	1.00	0.51	20	Dynamic
Stathopoulos et al. (2013)	0.67	0.77	30	Dynamic
	0.50	1.03	40	Dynamic
Computation procedure for the buildings in the current study according to NBCC 2015				
Current study	1.19	0.39	14.8	Static
	0.79	0.58	22	Dynamic
	0.54	0.77	29.2	Dynamic
	0.46	0.96	36.4	Dynamic
	0.37	1.15	43.6	Dynamic

Table 3: Original and transformed definition of shear and torsional coefficients in previous studies.

Study (Experimental)	Shear coefficient		Torsion coefficient	
	Original definition	Transformed definition	Original definition	Transformed definition
Isyumov and Case (2000)			$C_T = \frac{T}{q_H BLH}$	$C_T = \frac{T}{q_H BLH} \times \frac{H}{B} = \frac{T}{q_H B^2 L}$
Tamura et al. (2003)	$C_V = \frac{V}{q_H LH}$	$C_V = \frac{V}{q_H LH} \times \frac{H}{B} = \frac{V}{q_H BL}$	$C_T = \frac{T}{q_H LHR}$	$C_T = \frac{T}{q_H LHR} \times \frac{HR}{B^2} = \frac{T}{q_H B^2 L}$ $R = (B^2 + L^2)^{0.5} / 2$
Keast et al. (2012)	$C_V = \frac{V}{q_H LH}$	$C_V = \frac{V}{q_H LH} \times \frac{H}{B} = \frac{V}{q_H BL}$	$C_T = \frac{T}{q_H L^2 H}$	$C_T = \frac{T}{q_H H^2 L} \times \frac{H^2}{B^2} = \frac{T}{q_H B^2 L}$
Stathopoulos (2013)	$C_V = \frac{V}{q_H B^2}$	$C_V = \frac{V}{q_H B^2} \times \frac{B}{L} = \frac{V}{q_H BL}$	$C_T = \frac{T}{q_H B^2 L}$	$C_T = \frac{T}{q_H B^2 L}$

Figures

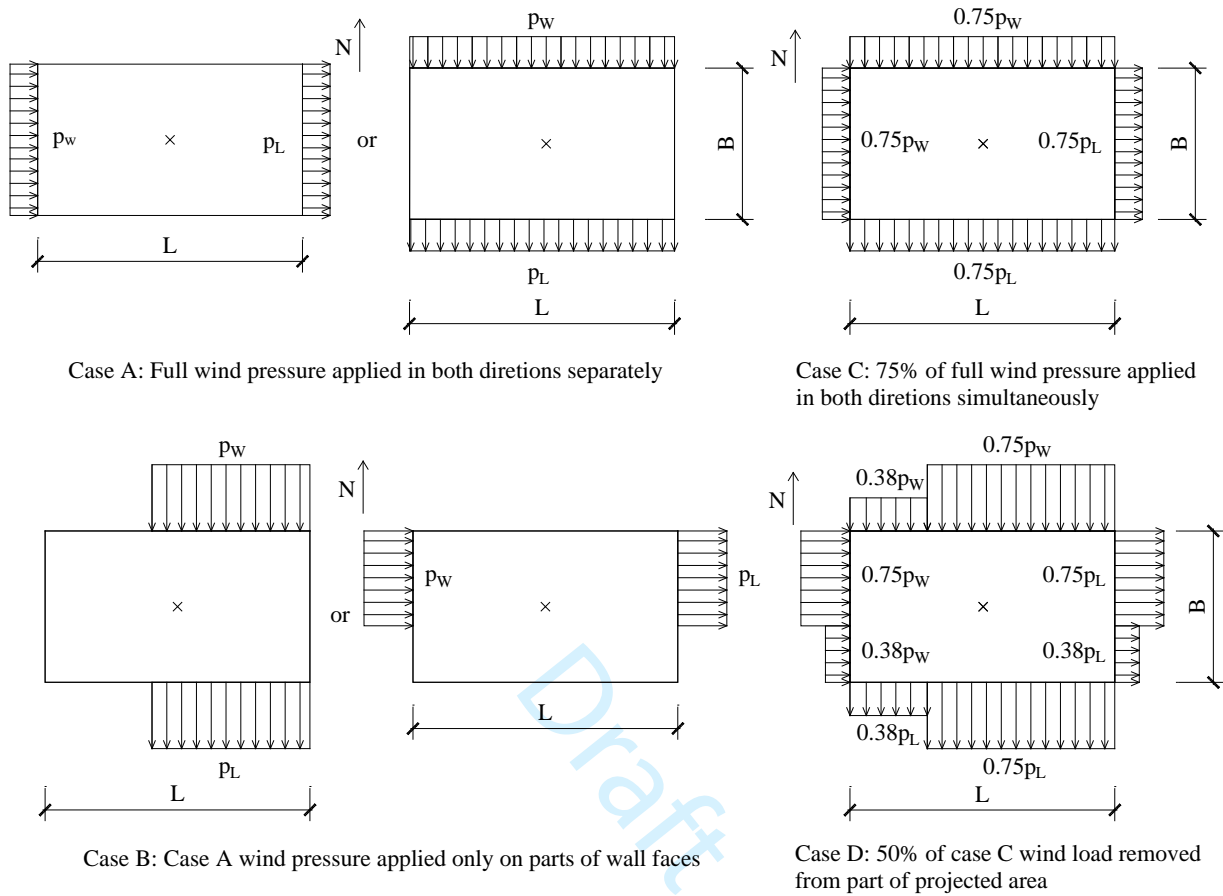
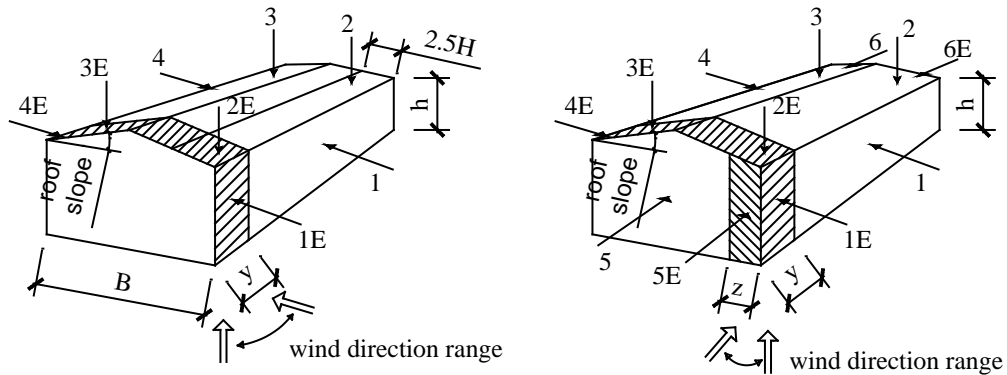


Fig. 1: Load cases for medium-rise buildings after NBCC 2015.



Load case A: winds generally perpendicular to ridge

Load case B: winds generally parallel to ridge

Roof slope	Building surfaces - Case A							
	1	1E	2	2E	3	3E	4	4E
0° to 5°	0.75	1.15	-1.3	-2.0	-0.7	-1.0	-0.55	-0.8

Roof slope	Building surfaces - Case B											
	1	1E	2	2E	3	3E	4	4E	5	5E	6	6E
0° to 90°	-0.85	-0.9	-1.3	-2.0	-0.7	-1.0	-0.85	-0.9	0.75	1.15	-0.55	-0.8

End-zone width y should be the greater of 6m or $2z$, where z is the gable wall end-zone defined for Load Case B below. Alternatively, for buildings with frames; the end-zone y may be the distance between the end and the first interior frame.

End-zone width z is the lesser of 10% of the least horizontal dimension or 40% of height, H , but not less than 4% of the least horizontal dimension or 1m.

Fig. 2: Load cases for low-rise buildings after NBCC 2015.

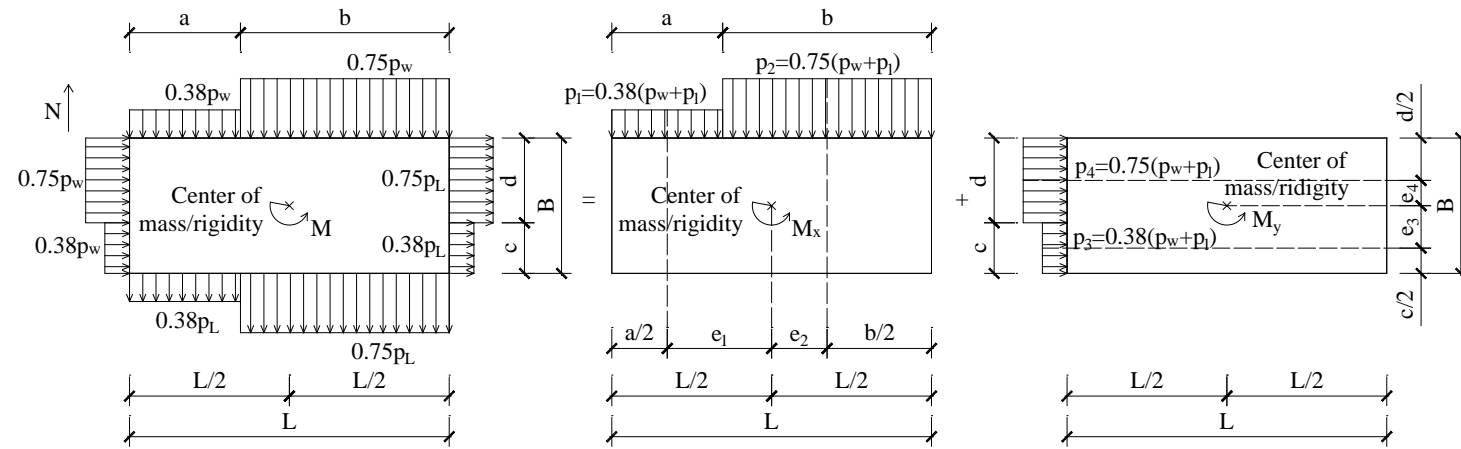
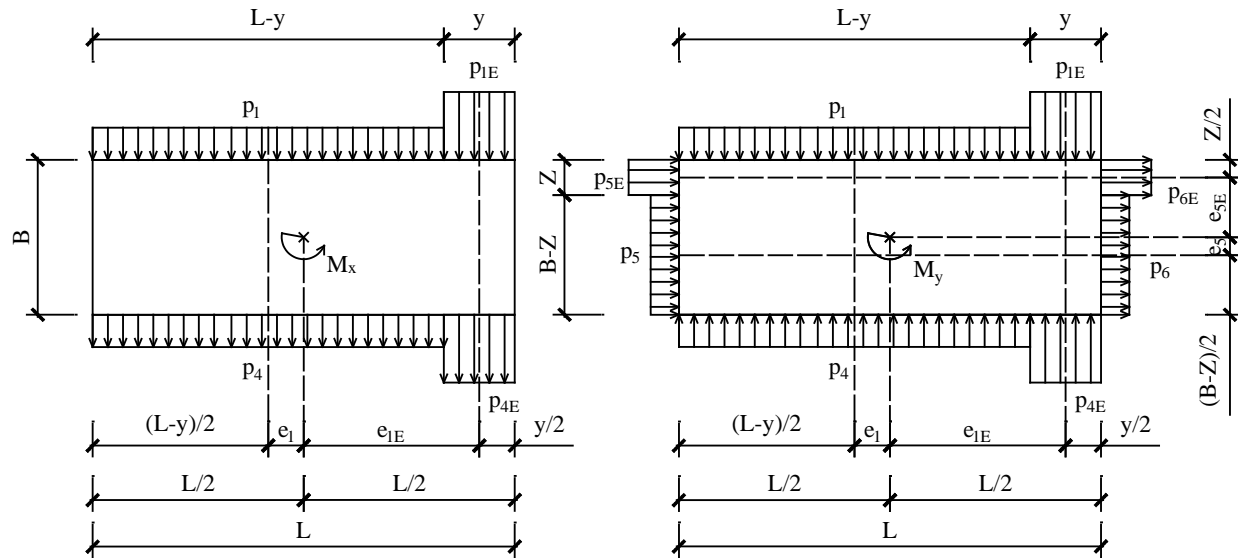


Fig. 3: Load Case D for medium-rise buildings analyzed in x and y directions.

Draft



Load case A: winds generally perpendicular to ridge

Load case B: winds generally parallel to ridge

End-zone width y should be the greater of 6m or $2z$, where z is the gable wall end-zone defined for Load Case B below. Alternatively, for buildings with frames; the end-zone y may be the distance between the end and the first interior frame.

End-zone width z is the lesser of 10% of the least horizontal dimension or 40% of height, H , but not less than 4% of the least horizontal dimension or 1m.

Fig. 4: Load cases for low-rise flat roof buildings according to NBCC 2015 provisions.

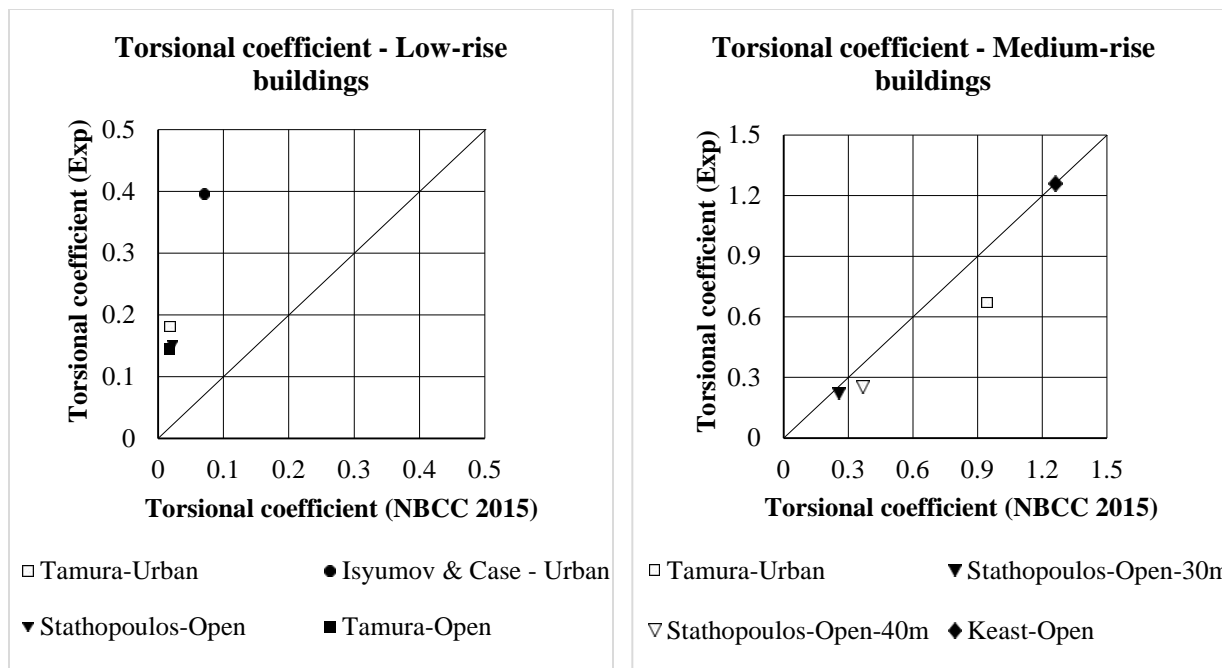


Fig. 5: Comparison of torsional coefficients for low-rise and medium-rise buildings in NBCC 2015 with experimental results from previous studies.

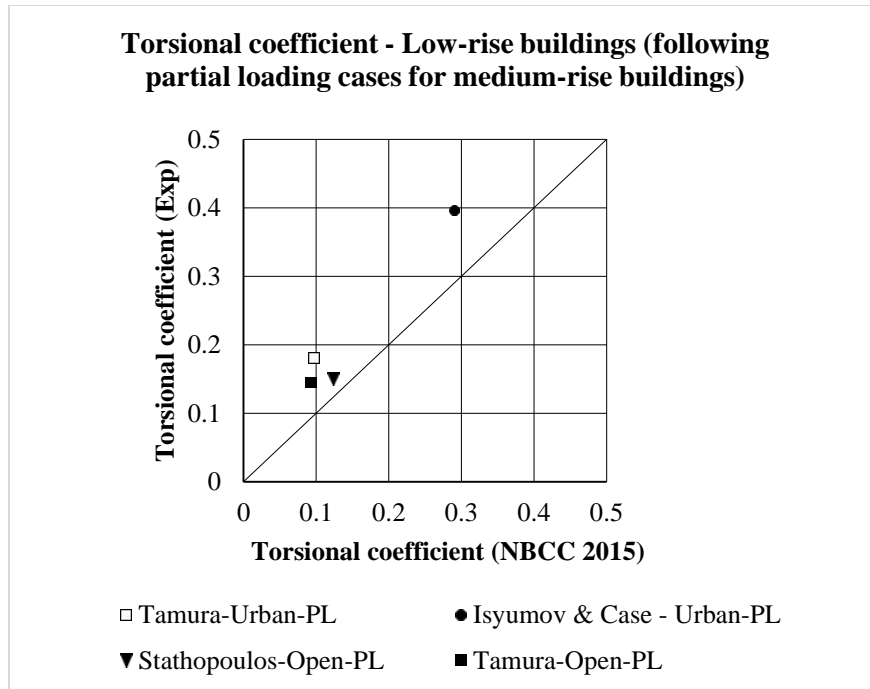


Fig. 6: Comparison of torsional coefficients for low-rise buildings in NBCC 2015 (following partial loading cases for medium-rise building, PL) with experimental results from previous studies.

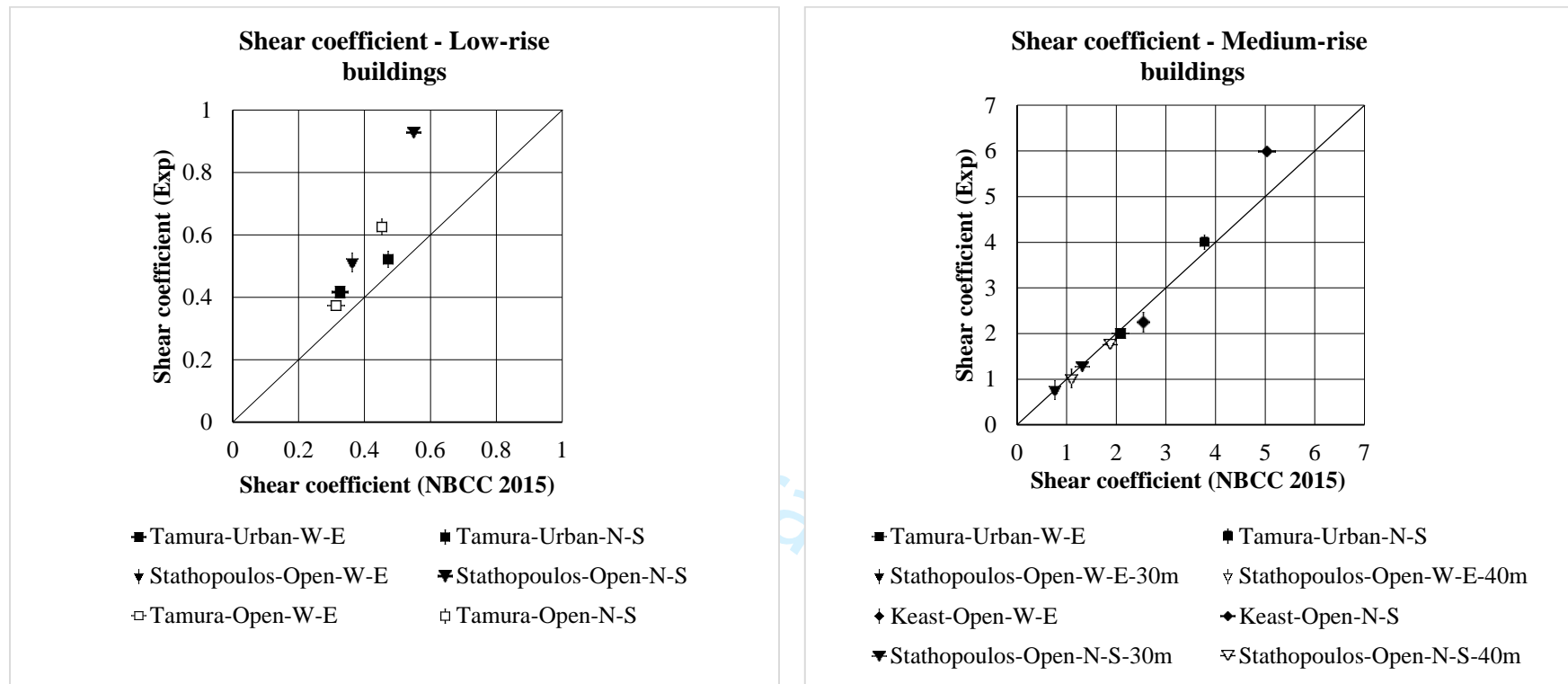
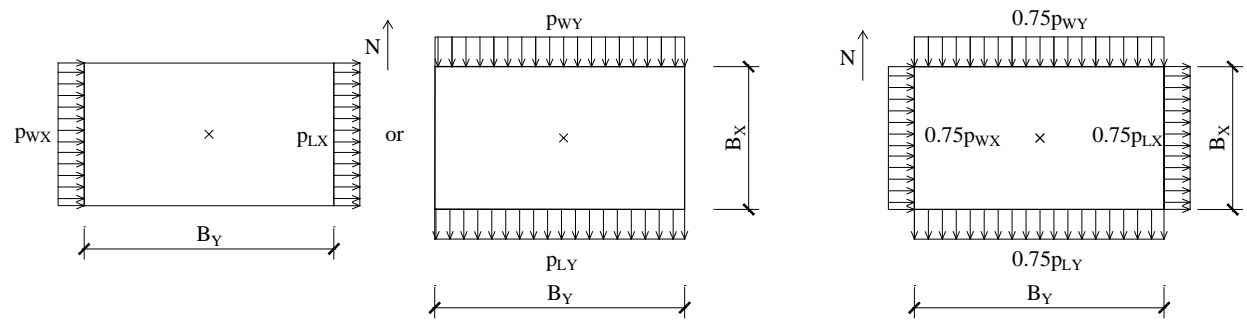
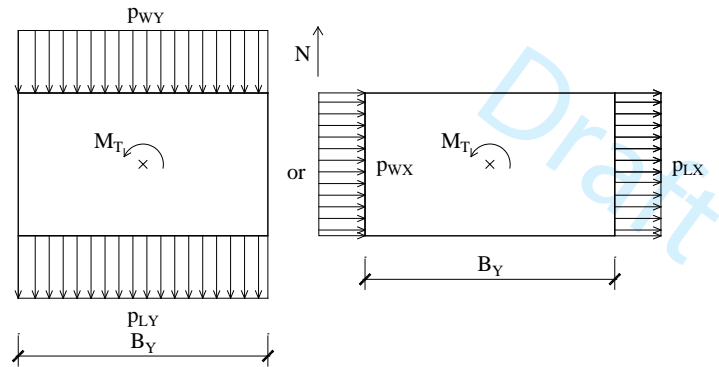


Fig. 7: Comparison of shear coefficients for low-rise and medium-rise buildings in NBCC 2015 with experimental results from previous studies.



Case 1: Full design wind pressure acting on the projected area perpendicular to each principal axis of the structure, considered separately along each principal axis.

Case 3: Wind loading as defined in Case 1, but considered to act simultaneously at 75% of the specified value.



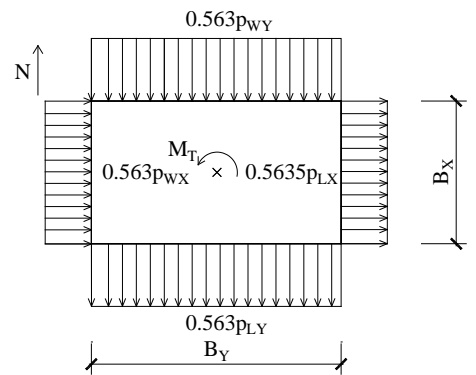
$$M_T = 0.75(P_{wX} + P_{lX})B_X e_X$$

$$e_X = \pm 0.15B_X$$

$$M_T = 0.75(P_{wY} + P_{lY})B_Y e_Y$$

$$e_Y = \pm 0.15B_Y$$

Case 2: Three quarters of the design wind pressure acting on the projected area perpendicular to each principal axis of the structure in conjunction with a torsional moment as shown, considered separately for each principal axis.

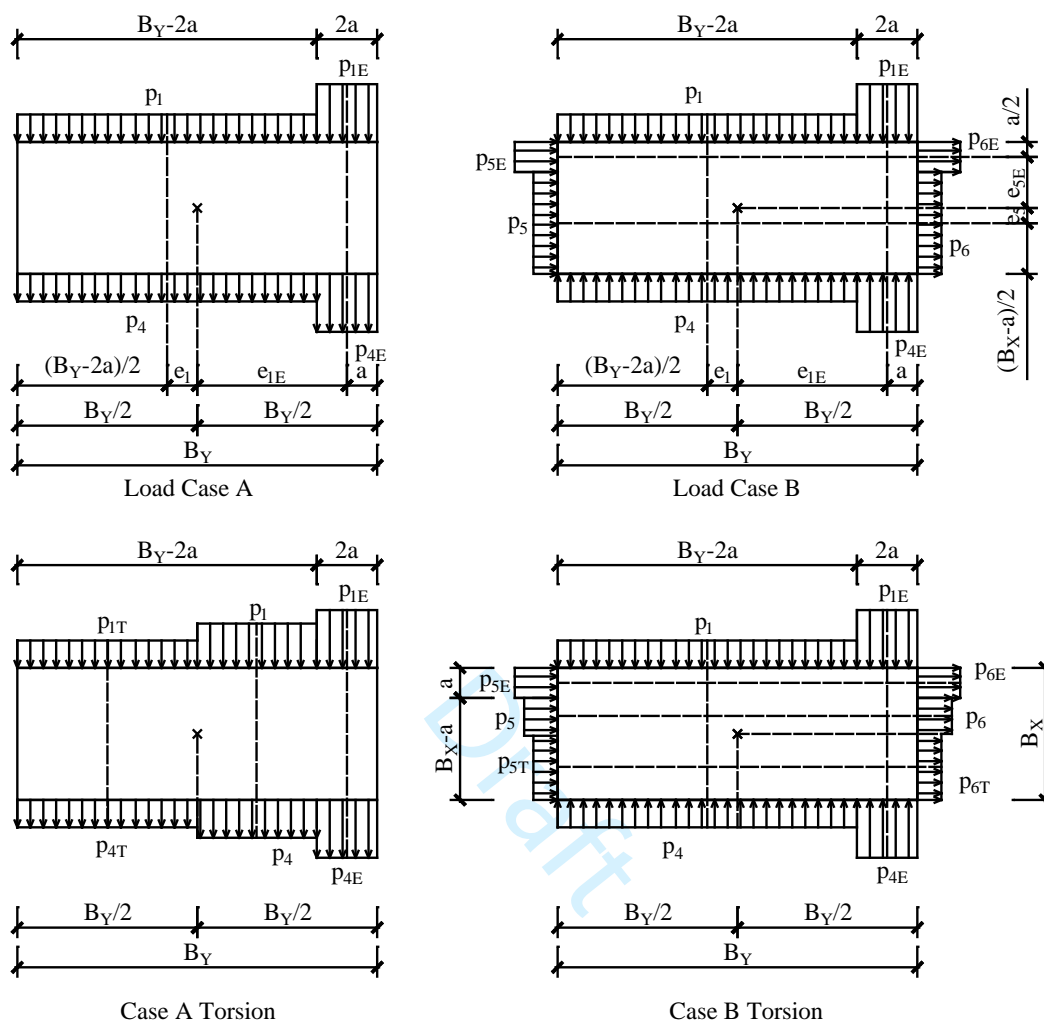


$$M_T = 0.563(P_{wX} + P_{lX})B_X e_X + 0.563(P_{wY} + P_{lY})B_Y e_Y$$

$$e_X = \pm 0.15B_X \quad e_Y = \pm 0.15B_Y$$

Case 4: Wind loading as defined in Case 2, but considered to act simultaneously at 75% of the specified value.

Fig. 8: Partial loading case for the Directional procedure after ASCE/SEI 7-10.



a: 10% of least horizontal dimension or 0.4h, whichever is smaller, but not less than either 4% of least horizontal dimension or 3ft (0.9m)

Fig. 9: Partial loading cases for the Envelope procedure after ASCE/SEI 7-10.

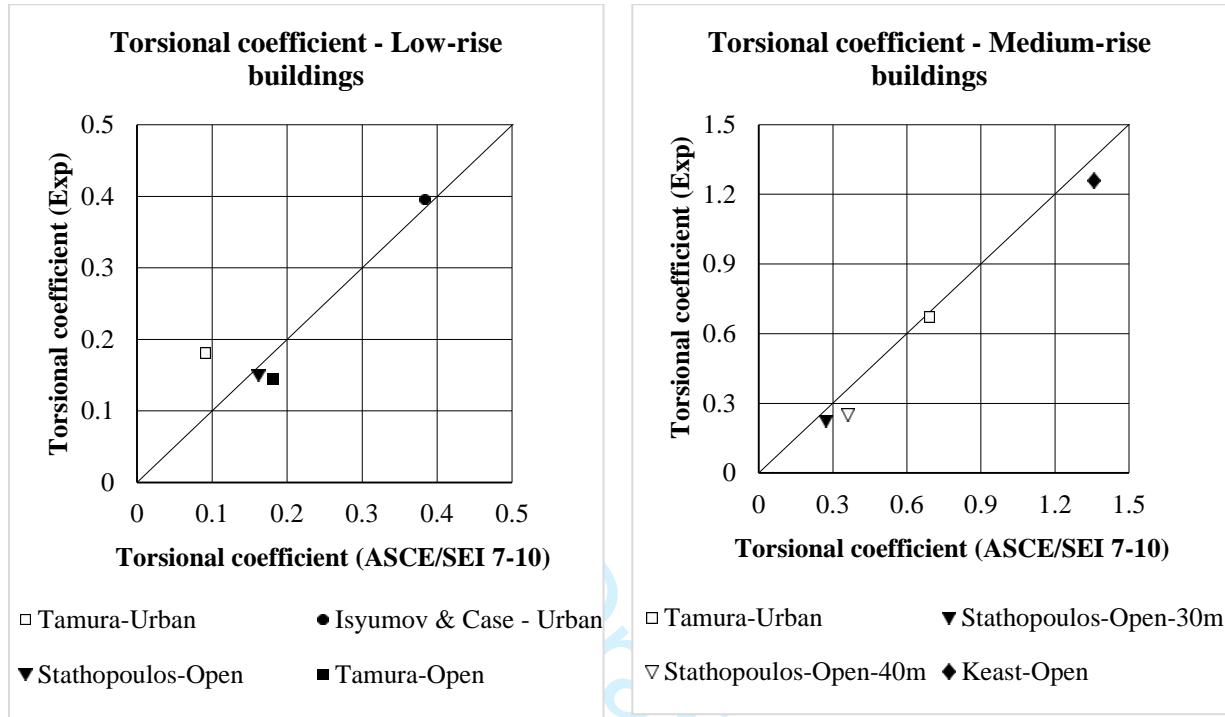


Fig. 10: Comparison of torsional coefficients for low-rise and medium-rise buildings in ASCE/SEI 7-10 with experimental results from previous studies.

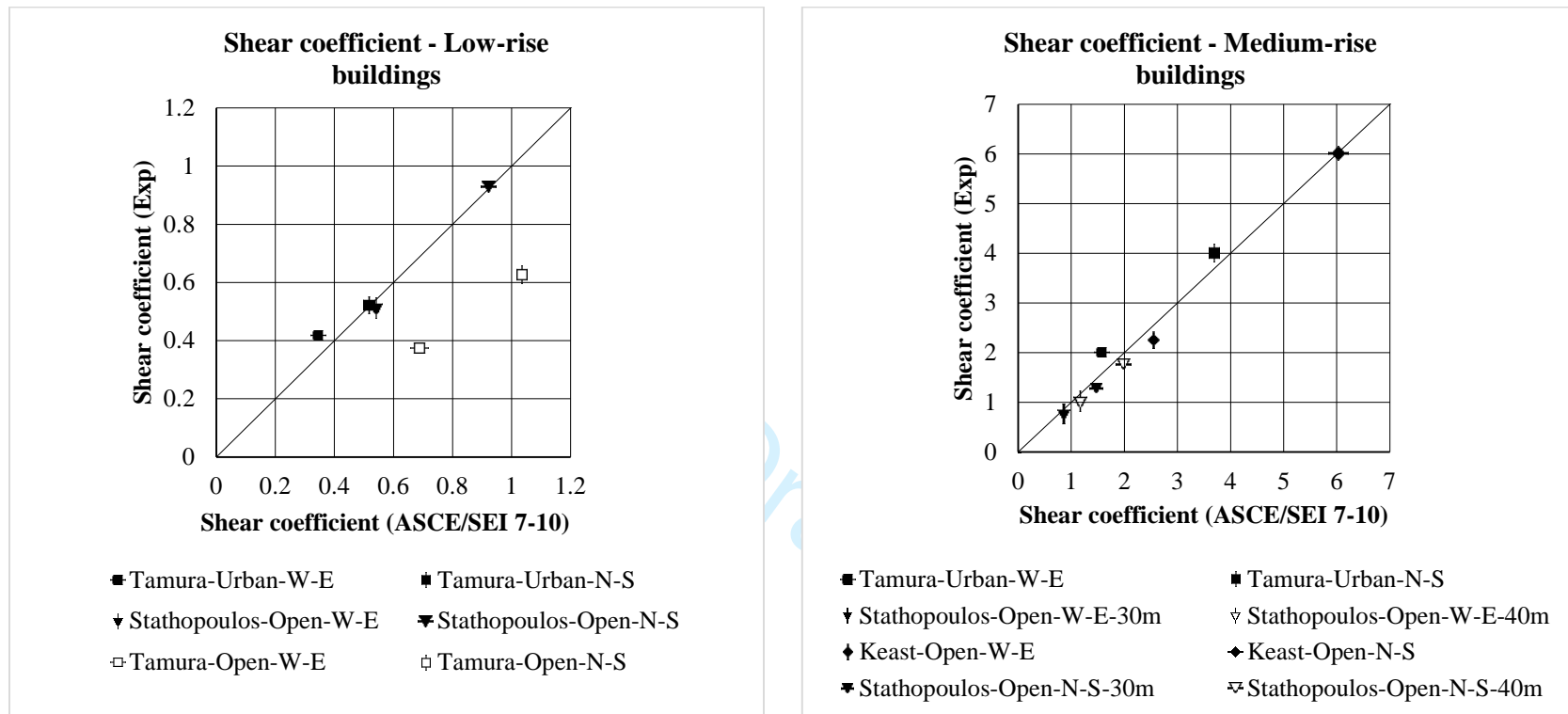


Fig. 11: Comparison of shear coefficients for low-rise and medium-rise buildings in ASCE/SEI 7-10 with experimental results from previous studies.

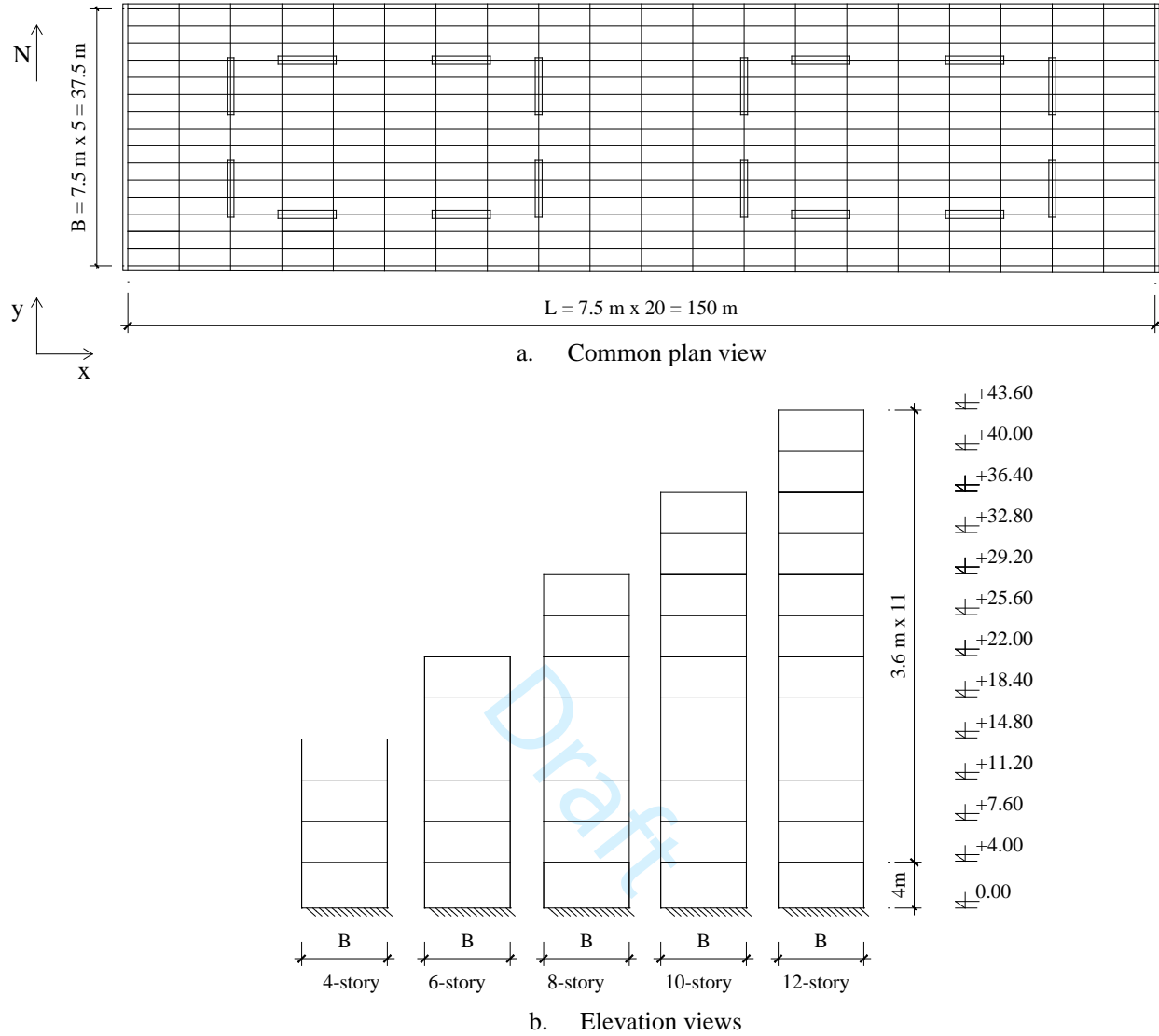


Fig. 12: Common plan and elevation views of the buildings in the current study.

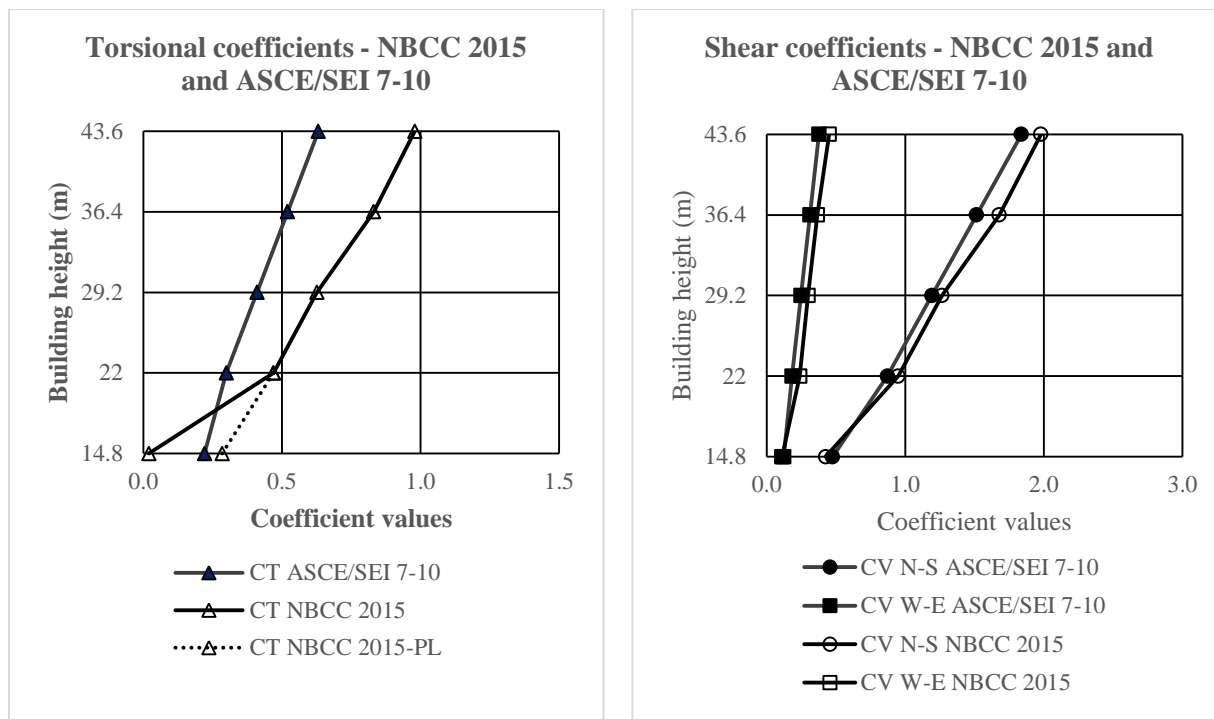


Fig. 13: Shear and torsional coefficients according to NBCC 2015 and ASCE/SEI 7-10.